

The material ratio of roadside backfill body based on spatiotemporal law of ground pressure: a case study of Xingtai Mine, China

Xinyuan Zhao (✉ 386308458@qq.com)

Anhui University of Science and Technology <https://orcid.org/0000-0001-5559-5839>

Xinwang Li

Hebei University of Engineering

Ke Yang

Anhui University of Science and Technology

Lichao Cheng

Hebei University of Engineering

Yiling Qin

Hebei University of Engineering

Research Article

Keywords: Spatiotemporal law, Gob-side entry retaining, Roadside backfill body, Material ratio

Posted Date: January 10th, 2022

DOI: <https://doi.org/10.21203/rs.3.rs-164754/v1>

License:   This work is licensed under a Creative Commons Attribution 4.0 International License. [Read Full License](#)

Abstract

The material ratio of the roadside backfill body in gob-side entry retaining determines its mechanical properties, which plays an important role in the supporting effect of the roadway surrounding rock. In this paper, a similar material modeling is used to verify the spatiotemporal law of the ground pressure in the engineering case of dense solid backfilling mining in Xingtai Mine, China. Based on that law, the theoretical requirements for the bearing performance of the roadside backfill body are proposed. Finally, a material ratio that meets the theoretical requirements is obtained by compression test, and the deformation and failure characteristics of the backfill body with this ratio are analyzed. The results show that the maximum pressure of the backfill body measured in Xingtai Mine is 5.5 MPa, which is about 40 m away from the coal face, after 40m, the pressure of the backfill body will not increase anymore. The similar simulation test also proved that the ground pressure behind the coal face increases gradually and tends to be stable during the backfilling process, which shows certain spatiotemporal characteristics. Through the proportioning experiment, it is determined that the optimal material ratio of the roadside backfill body is gangue: fly ash: cement = 10:3:1, which meets the theoretical requirement that the strength of the roadside backfill body at any position is not less than the ground pressure at that position. The research results provide a reference for the engineering practice of gob-side entry retaining in dense backfilling mining.

1. Introduction

The dense solid backfilling mining technology has been widely used, which can effectively control the movement of the overlying strata in the goaf, reduce the degrees of the ground pressure behavior in the stope, and can provide good conditions for gob-side entry retaining (Miao et al. 2008; Huang et al. 2017). Retaining roadways along the edge of the backfilling area is an innovative combination of gob side entry retaining technology based on the application of solid waste backfill materials in goaf, which has the dual advantages of backfilling mining and gob-side entry retaining. It can not only deal with a large amount of solid waste, protect the surface environment, but also reduce roadway excavation. Therefore, this method has significant technical advantages and economic benefits (Yang et al. 2019; Li et al. 2019; Zhang et al. 2012).

In the research field of gob-side entry retaining in solid backfilling mining, many experts and scholars have conducted in-depth research on it mainly from two aspects, namely, the surrounding rock control of gob-side entry retaining in backfilling mining and the material properties of roadside backfill in gob-side entry retaining. Research on surrounding rock control of gob-side entry retaining in backfilling mining, Zhang *et al.* (2013) analyzed the deformation characteristics of surrounding rock of gob-side entry retaining in dense backfilling mining and the action mechanism of roadside backfill body, established the relationship between lateral pressure and reasonable width of roadside backfill body; Ju *et al.* (2015) proposed the concept of a collaborative control system for overlying strata under the condition of backfilling mining and retaining roadway, and determined the parameters of influencing factors of surrounding rock stability by numerical simulation; Xie *et al.* (2014) proposed the comprehensive control technology of high-water backfill material performance optimization, rockbolt-cable combined support and hydraulic support combined support under the conditions of deep and large height backfilling mining, and explained its

mechanism. Ma *et al.* (2011) established a mechanical model for the key stratum of gob-side entry retaining in fully-mechanized backfilling mining, adopted Coulomb's earth pressure theory to solve the problem of lateral pressure of the gangue backfilling area on the supporting wall beside the roadway. In addition to the surrounding rock control of gob side entry retaining in backfilling mining (Zhou et al. 2012; Guo et al. 2017; Huang et al. 2011), many scholars (Cheng et al. 2020; Sun et al. 2019; Yang et al. 2017) have also studied the mechanical properties of the roadside backfill body. For example, Chang *et al.* (2018) analyzed the interaction mechanism between the roof and the roadside backfill body in gob-side entry retaining according to the elastic thin plate theory of stope roof, studied the stress state and mechanical response of the roadside backfill body, and used high-water materials as the roadside backfill body for field application; Gong *et al.* (2018) studied the effects of the water-cement ratio, aggregate content, and age on the contractibility and resistance increasing speed, compressive strength, and postpeak carrying capacity of the concrete with gangues as an aggregate, also discussed the rationality and adaptability of gangue concrete as an RSB (roadside support body) material for backfilling GER (gob-side entry retaining); Li *et al.* (2017) analyzed the strain hardening behavior of crushed gangue backfill materials through compaction test, and proposed a method of simulating CGBM (crushed gangue backfill materials) using double yield model. However, when gob-side entry retaining is carried out in the backfilling mining engineering, the roadside backfill body is often damaged due to its strength that cannot support the roof pressure, resulting in serious roadway deformation and damage, and high safety risks. If the support strength of the roadside backfill body is increased blindly, the cost of the roadside backfilling will rise sharply, the benefit of retaining the roadway will decrease, and the application of gob side entry retaining in backfilling mining will be restricted. The bearing capacity of roadside backfill body often does not match with the ground pressure strength of gob side entry retaining, there is no good solution in the current open literature. Therefore, it is necessary to conduct a study on optimizing the ratio of the roadside backfill materials based on the spatiotemporal law of ground pressure, so as to solve the adaptability problem between the bearing capacity of backfill materials and the ground pressure behavior of gob side entry retaining.

In this paper, Xingtai Mine is taken as an engineering practice to monitor the ground pressure, and the similar material simulation method is used to verify the spatiotemporal law of ground pressure behavior in dense solid backfilling mining, thereby establishing the spatiotemporal coupling model of roof and the backfill body, and the theoretical requirement that the bearing performance of the roadside backfill body meets the ground pressure behavior is put forward. Finally, through the material selection and compression experiment, the material ratio of the roadside backfill body that meets the theoretical requirements is obtained. This paper provides a theoretical direction to solve the adaptability problem between the bearing capacity of the roadside backfill body and the ground pressure behavior of gob-side entry retaining, which has a reference significance for the engineering application of gob-side entry retaining in backfilling mining.

2. Engineering Practice

2.1 Coal face overview

The engineering practice of backfilling mining in Xingtai Mine of China is selected as an example for analysis. Comprehensive mechanized solid backfilling mining technology with gangue and fly ash as the

main backfill materials is adopted in the coal face. After the goaf is filled with solid waste, the tamping mechanism at the back of each hydraulic support is used to repeatedly compact the backfill materials, so that the goaf can achieve a dense backfilling effect. According to relevant literature (Liu et al. 2010) and on-site survey, the average dip angle of the coal seam where the coal face of Xingtai Mine is located is 9°, the average buried depth is 320 m, and there is a thin layer of gangue in the middle of the coal seam. The average mining height of the coal face is 3.0 m, the inclined length is 50 m, and the total advancing length is about 133 m. The actual backfill operation takes about 40 days, and the maximum daily advancing distance is 4.8 m.

Through the judgment and analysis of the rock samples collected on-site, it is found that the lithology of the roof and floor of the coal seam where the coal face is located is mainly sandstone and shale with different thicknesses. According to the relevant Chinese standards for rock classification and field nomenclature (GB/T 17412.2-1998), sandstone is divided into fine sandstone (grain size: 0.25-0.063mm), medium sandstone (grain size: 0.5-0.25mm) and coarse sandstone (grain size: 2-0.5mm) by grain size. The shale is named carbonaceous shale and sandy shale according to the different substances mixed in the shale. If the shale contains a large amount of carbonized organic material, it is called carbonaceous shale, and if the shale is mixed with a certain amount of sandy material, it is called sandy shale. Therefore, the upper and lower strata lithology of the coal face is shown in Table 1.

Table 1 Lithology and description of upper and lower strata of the coal face

No.	Rock stratum	Average thickness/m	Lithology description
1	Fine sandstone	8	Gray, with mica, clay cement.
2	Carbonaceous shale	6	Contains a large amount of dispersed carbonized organic matter, black
3	Fine-grained sandstone	10	The weathered surface is yellowish-brown, the fresh surface is grayish-green, fine-grained structure and massive structure
4	Coarse-grained sandstone	12	Light gray, coarse sand structure, massive structure, the main minerals are quartz, feldspar, mica, etc.
5	Sandy shale	8	Light gray, containing a lot of plant fossil fragments.
6	Medium sandstone	6	Light gray, mainly composed of quartz feldspar, clear bedding.
7	Sandy shale	7	Gray-black, containing plant fossils, partially containing bauxite.
8	Fine sandstone	9	Gray, with mica, clay cement.
9	Sandy shale	4	Black, with plant fossils, and a lot of mud.
10	Coal seam	3	Black powder, good coal quality, containing plant fossils.
11	Sandy shale	6	Dark gray, thin layer, rich in plant fossils, mainly muddy, with the squeezed bottom.
12	Fine sandstone	4	Gray, hard, horizontally layered.

2.2 Monitoring results of ground pressure

Online monitoring machines are arranged on the hydraulic supports along the inclination of the coal face to monitor the variation law of the working resistance of the hydraulic support during the advancing process of the coal face. The monitoring results show that as the coal face advances, the first weighting of the roof is not obvious, and the strength of the periodic weighting is weak. The support pressure of the coal face is overall low, which is less than the rated working resistance. The pressure distribution along the inclination of the coal face is different with the compactness of the backfill body, and the roof pressure is small in the place with high backfill density. The pressure peak appears at a periodic step of 40-55 m, and the pressure strength coefficient is about 1.15, indicating that the goaf backfill body effectively controls the movement of the overlying strata and weakens the strength of ground pressure behavior at the coal face.

When the coal face advances 15 m, 40 m, and 65 m from the open-off cut, three rows of pressure sensors are embedded in the goaf backfill body to monitor the backfill body pressure. The monitoring results show that the pressure monitor has a pressure display in the range of 13-15 m behind the coal face. When the span length of the main roof (about 15 m) is reached, the overlying strata subsidence faster and the backfill

body is rapidly compressed. When the distance from the coal face is 15 m, the pressure monitored on the backfill body is 3.5 MPa, while the pressure reaches the peak value of 5.5 MPa when the distance is 40 m from the coal face, and then the pressure tends to be stable, which indicates that as the advancing distance increases, the force of the backfill body increases first and then stabilizes.

3. Similar Material Modeling

To verify the spatiotemporal law of ground pressure behavior in the engineering practice of dense backfilling mining in Xingtai Mine, deeply study the spatiotemporal characteristics of coupling effect between the roof and dense backfill body in backfilling mining, and provide guidance for the selection and optimization of roadside backfill materials, the similar material model was established and the similar material simulation test was carried out.

3.1 Construction process of similar material model

The size of the similar material model in this experiment is 1.5 m×0.1 m×0.85 m (length×width×height), the bulk density similarity ratio of similar materials and rocks is 1:1.6 (model: prototype), the parameters such as geometric similarity ratio, stress similarity ratio, and time similarity ratio are calculated by referring to the equations in the literature, respectively. Finally, combined with the laboratory conditions, it is determined that the geometric similarity ratio suitable for the model is 1:100 (model: prototype), the stress similarity ratio is 1:160 and the time similarity ratio is 1:10. Fine sand, lime and gypsum are used as materials for simulating the rock stratum in the similar material model. The particle size distribution curves of similar materials with different ratio numbers are shown in Fig.1. It can be found that the grain size distribution of similar materials with different proportion numbers has little difference. The maximum grain size of similar materials is about 1800 μm and the minimum grain size is about 0.3 μm. The volume proportion of similar materials with a grain size of about 425 μm is the largest, more than 6%.

The thickness of the rock stratum in the model is determined by the actual thickness of the rock stratum and the geometric similarity ratio. The material consumption of each rock stratum in the similar material model is calculated by Equation (1).

$$W = kabhp \quad (1)$$

Where, W is the amount of material used for each rock layer, kg; k is the surplus coefficient, generally 1.2-1.3; a , b and h are the length, width and height of similar material simulation test bench, m; ρ is the density of similar material, taking 1650 kg / m³.

The amount of each material in each rock stratum is determined by the total amount of material and the ratio number in each rock stratum. The water consumption of each rock stratum is determined according to 10% of the material dosage, and the material ratio of rock stratum in the mode is finally determined, as shown in Table 2.

Table 2 Material ratio of rock stratum in the model

Serial number	Strata name	Strata thickness/cm	Ratio number	Fine sand/kg	Lime/kg	Plaster/kg	Water/ml
1	Fine sandstone	4	755	9	0.64	0.64	1028
2	Sandy shale	6	655	12.5	0.42	0.42	1334
3	Coal seam	3	873	8	0.7	0.3	900
4	Sandy shale	4	855	9	0.56	0.56	1012
5	Fine sandstone	9	755	21	1.5	1.5	2400
6	Sandy shale	7	873	17	1.49	0.64	1913
7	Medium sandstone	6	655	14	1.17	1.17	1634
8	Sandy shale	8	855	18	1.13	1.13	2026
9	Coarse-grained sandstone	12	755	28	2	2	3200
10	Fine-grained sandstone	10	855	23	1.44	1.44	2588
11	Carbonaceous shale	6	955	12.5	0.69	0.69	1388
12	Fine sandstone	8	755	18	1.29	1.29	2058

3.2 Selection of similar materials for backfill blocks

To more truly reflect the deformation law of overlying strata in the stope during the solid backfilling mining process, according to the similarity principle, the compression characteristic curve of the simulated backfill body should be similar to that of the actual backfill body composed of gangue and fly ash, so as to ensure the accuracy of dynamic deformation of similar simulation materials in the process of model excavation and backfilling. Combined with laboratory conditions, four combinations of soft and hard foam materials with different thickness ratios were selected for compression experiments to find suitable similar materials for backfill bodies. Four combinations of soft and hard foams with different thickness ratios are respectively No. 1 material combination with soft foam: hard foam=0:1, No. 2 material combination with soft foam: hard foam=1:0, No. 3 material combination with soft foam: hard foam=1:2, No. 4 material combination with soft foam: hard foam=1:3. The composition of the four combined materials and their compression curves are shown in Fig.4.

3.3 Simulation and monitoring scheme

When building the model, a micro pressure cell was arranged at every 10 cm interval in the rock stratum about 5 cm above the coal seam, and was respectively numbered "R1-R10". Two micro pressure cells, coal

pillar 1 and coal pillar 2, numbered "P1" and "P2", were respectively arranged at the junction of the coal seam and the immediate roof at a distance of 10 cm from the model boundary. According to the field practice and experimental needs, the coal seam was excavated and backfilled after the model was applied with compensation load and remained for 15 minutes. 20 cm coal pillars are reserved on both sides of the model, and 110 cm in the middle is the excavation and backfill range. The direction of excavation and backfilling is from left to right. The specific layout of the measuring points is shown in Fig.5.

In the experiment, each backfill block is used to represent the actual daily backfilling step on site. According to the average daily backfilling distance in engineering practice, the average width of the backfill block is set to be 3.3 cm, that is, every 3.3 cm of excavation is filled with a backfill block. For every three blocks filled, a pressure cell was arranged in the middle backfill block to measure the force on the backfill body. The number of the backfill body where the pressure cell was arranged is "ct1-ct11". According to the on-site backfilling process, the coal seam is excavated for a block width and then filled with a backfill block. Wait for the model to stand for 5min, excavate and backfill again, follow this cycle until the stopping line. During the excavation and backfill process, the DH3815N static strain test system was used for collecting data regularly, the interval was 5 s. And XJTUDP three-dimensional optical photogrammetry system was used to take pictures every 10 cm of backfilling. After the excavation and backfill are completed, wait for the model to balance and stop collecting data. Finally, the model was allowed to stand for 12 hours and then the movement law of overlying strata was observed with XJTUDP three-dimensional optical photogrammetry system.

3.4 Spatiotemporal law of stress on roof and backfill body

Through monitoring and recording the data of each measuring point in the process of coal seam excavation and backfilling, the stress data of each measuring point under the relative time of test record are obtained, which is plotted as shown in Fig.6 and Fig.7.

As can be seen from Fig.6 that in the excavation and backfilling process of the coal seam, the stress of the roof measuring point has experienced the changing process of "stress rise-stress unloading-stress recovery and then stress stability". From this analysis, before the coal face passes through each roof measuring point, the roof measuring point is in the area of the coal face's advanced abutment pressure, which causes the stress of the measuring point to increase. As the range of mining and backfilling expands, the peak stress of advanced coal face also shows a slowly increasing trend, and its peak value tends to be stable after passing through the measuring point R8, at this time the backfilling distance is more than 80 cm; When the coal face passes under each roof measuring point, the immediate roof loosens and the stress of each measuring point drops sharply; After the coal face passes the roof measuring point about 3-5 backfill blocks, the roof stress begins to recover slowly, which indicates that the strata above the roof measuring points are bent, subsided and overlapped; After excavation and backfilling are completed, the stress of roof measurement points is finally stabilized between 10-23 kPa, showing the stress distribution with high in the middle of the backfilling area and low near the coal pillar. The measured stress value of the roof after stabilization is less than the theoretical value of the in-situ rock stress. The reason is that there is one or more key stratum in the overlying strata. The key stratum is not completely broken during the

advancement of the coal face, which has taken part of the overlying strata's weight and transferred the overlying stress to both coal pillars. The stress of measuring points on both coal pillars slowly increases with the increase of the backfilling time and distance. The stress of P1 measurement point begins to stabilize after backfilling 100cm, and the stabilized stress value is about 68 kPa, which exceeds the theoretical value of the in-situ rock stress.

In Fig.7, the stress of each measuring point on the backfill body shows a trend of first increasing and then stable with the increase of backfilling time and distance. During the backfilling process, it is found that 1-2 backfill blocks behind the coal face are basically not stressed, and the stress of backfill blocks at about 3-6 cm behind the coal face begins to increase. As the distance from the coal face increases, the force of the backfill block increases accordingly until it stabilizes. The distance between the initial stress and the stress stability of the backfill block is about the width of 6-8 backfill blocks. After the stress of each measuring point is stable, the value is in the range of 10-25 kPa, the stress of the backfill body measuring point in the middle of the backfilling area increases faster, and its final value is generally larger than that of the measuring point near the coal pillar. The stress distribution of the backfill body is basically consistent with that of the roof measuring point. The stress distribution and growth law of the backfill block are basically consistent with the stress monitoring results in engineering practice.

From the comparative analysis of Fig. 6 and 7, it can be found that the stress of the backfill body measuring point begins to increase slowly after the stress of the roof measuring point decreases rapidly, which indicates that the interaction between the roof subsidence and the support of the backfill body occurs at this time. The support effect of the backfill body on the roof increases with the increase of the backfilling distance, and the roof stress begins to recover slowly until the supporting force of the backfill body and the roof subsidence stress reach the equilibrium state. This phenomenon shows that there is a coupling characteristic between roof subsidence and backfill body support within a certain distance behind the coal face.

3.5 Spatiotemporal law of displacement on roof and backfill body

To show the spatiotemporal law of the roof and backfill body in displacement, three-dimensional dynamic deformation diagrams of the model after backfilling 0 cm, 20 cm, 40 cm, 60 cm, 80 cm, 100 cm, 110 cm and standing for 12 hours after stopping mining are selected, as shown in Fig.8a-h.

As can be seen from Fig.8a-h, when the coal seam is not excavated and backfilled, overlying strata in the model basically has no displacement; When the backfilling distance is 20cm, the overlying strata in front of and behind the coal face begins to subside and deform slightly, and the subsidence is less than 1 mm; The maximum subsidence of the roof after backfilling 40 cm, 80 cm, and 110 cm is 1.299 mm, 2.166 mm, 3.465 mm, respectively, which indicates that as the coal face advances, the backfilling distance increases, bending and subsidence of the roof in goaf are gradually obvious. The area with the greatest degree of roof subsidence is located in the middle of the excavation and backfilling range, and the roof subsidence on both sides of the backfilling area is small due to the support of the coal pillar. The distribution of the

compression degree of the backfill body can also be reflected from the stress value of the backfill body after stabilization in Fig.7.

The roof subsidence and backfill body compression are not only shown in the spatial distance, but also temporality. Comparing the deformation diagrams of 110 cm backfilling and standing for 12 hours after stopping mining, it is found that although the excavation and backfilling work of the model has been completed, the deformation of the rock stratum has not stopped. The maximum subsidence of overlying strata in the model with backfilling of 110 cm and standing for 12 hours is 3.465 mm and 4.331 mm respectively. As time goes on, the interaction behavior of the overburden subsidence and the compression of the backfill body is still proceeding slowly and smoothly until the supporting force of the backfill body can resist the pressure of the roof subsidence, which reflects the temporality of roof subsidence and strength increase of backfill body.

4. Theoretical Requirements For The Bearing Performance Of The Roadside Backfill Body

According to engineering practice and similar material modeling, the spatiotemporal model of roof subsidence and strength increase of the backfill body is established, as shown in Fig.9. Along the coal face strike, as the backfilling distance increases and time passes, the subsidence state of the roof behind the coal face gradually develops from the active stage to the stable stage, the overburden pressure on the backfill body gradually increases and then stabilizes as it moves away from the coal face. Under the action of the roof load, the supporting strength of the backfill body has also undergone the process of slow growth and then stabilization. The roof at any distance behind the coal face will produce pressure on the backfill body due to its subsidence, and the time taken for the coal face to pass through this distance is also the period when the support strength of the backfill body increases continuously. Therefore, the law of ground pressure behavior and the strength growth of the backfill body show certain spatiotemporal coupling characteristics (Li et al. 2020).

Based on the spatiotemporal law of ground pressure behaviors, the gob-side entry retaining in dense backfilling mining, theoretically needs to meet the requirement that behind the coal face, the support strength of the roadside backfill body increasing with the advancing time of the coal face is always not less than the ground pressure varying with the advancing distance of coal face, that is to say, during the advancing process of the coal face, the supporting strength of the roadside backfill body at any distance behind the coal face is always not less than the roof pressure at that place, including when the roof pressure reaches the peak value behind the coal face, the support strength of roadside backfill body is still not less than this peak value. The formula is expressed as:

$$\sigma_x \leq \sigma_t \quad (2)$$

Where σ_x is the roof pressure at any place behind the coal face; σ_t is the supporting strength of the backfill body at the same place.

Meanwhile, the compression of the roadside backfill body should not be too large to ensure the requirements of the roadway section. Assuming that the initial section of the roadway is rectangular, after the immediate roof tilts and subsides, the compressed area of the roadway is similar to a right angle trapezoid, as shown in Fig.10.

$$S_a - \frac{L(b+c)}{2} \geq S_r \quad (3)$$

Where S_a is the initial cross-sectional area of the roadway; L is the width of the roadway; b is the compression amount of the roadside backfill body; c is the compression amount on one side of the coal seam; S_r is the cross-sectional area of the roadway specified by coal mine safety regulations.

In this way, during the backfilling process, the roadside backfill body and the goaf backfill body jointly control the deformation of the surrounding rock and the movement of the overlying strata, and it can always maintain stability and integrity, and achieve the effect of effectively supporting and maintaining the roadway (Chen et al. 2018).

5 Material Ratio Test Of Roadside Backfill Body

5.1 Selection of gangue gradation

The literature (Xu et al. 2011) pointed out that loose gangue has the least compactness in its natural state (original gradation). Therefore, according to the particle size distribution of the gangue discharged from mine production, the gangue with a particle size of less than 40 mm is selected as the test material, and Talbol Formula (Fuller et al. 1907) is used to guide the gangue gradation. Talbol Formula is as follows:

$$P = 100\left(\frac{d}{D}\right)^n \quad (4)$$

where P is the percentage passing different sieve sizes, %; d represents the particle size of the gangue, mm; D is the maximum particle size of the gangue, mm; n is Talbol coefficients, generally between 0.3 and 0.7. The proportion of continuous gradation gangue can be obtained by sieving the gangue with particle sizes less than 40 mm, as shown in Table 3.

Table 3 Gangue gradation with different Talbol coefficients

n	The proportion of gangue in different particle sizes/ %			
	0 – 10 mm	10 – 20 mm	20 – 30 mm	30 – 40 mm
0.3	65.98	15.25	10.5	8.27
0.4	57.43	18.36	13.34	10.87
0.5	50	20.71	15.89	13.40
0.6	43.53	22.45	18.17	15.85
0.7	37.89	23.67	20.2	18.24

The stress-strain curve of the continuous gradation gangue was obtained by compression test with different Talbol coefficients (as shown in Fig.11).

Fig.11 shows that the compressive stress-strain curve of continuously graded gangue exhibits a logarithmic pattern that increases rapidly and then increases slowly, the inflection point is found at about 2 MPa. By comparing the stress-strain curves with different Talbol coefficients, it is found that the strain variation of continuous gradation gangue with Talbol coefficient $n = 0.4$ is the smallest, indicating that the compression ratio of continuous gradation gangue with Talbol coefficient $n = 0.4$ is the smallest and the density is the highest, this gradation is therefore chosen as optimal for use as aggregate in the test material.

5.2 Test scheme

To find a material ratio that can make the aging strength of the roadside backfill body meet the spatiotemporal law of ground pressure behavior under the dense backfilling condition, make the roadside backfill body has enough strength to support the roof pressure and movement in time, which play the role of maintaining the roadway section. Considering the backfilling cost, gangue, fly ash and cement were selected as test materials (as shown in Fig.12), and then specimens were made and compressed. The specific ratio scheme is shown in Table 4.

Table 4 Material ratio scheme of roadside backfill body

Test number	Test materials	Ratio
1	Gangue: Fly ash	10:3
2	Gangue: Cement	10:0.5
3	Gangue: Cement	10:1
4	Gangue: Fly Ash: Cement	10:3:0.5
5	Gangue: Fly Ash: Cement	10:3:0.75
6	Gangue: Fly Ash: Cement	10:3:1

It should be noted that the water-cement mass ratio of the specimens is 0.6. The material is evenly stirred and poured into the forming mold and then compressed vertically, the compressive stress is 2 MPa to

simulate the tamping force of hydraulic support on the backfill body during the on-site backfilling. The compacted specimens are placed under natural conditions (the average temperature is about 25°C, the relative humidity is about 80%), and demoulding after one day. In the above-mentioned engineering practice, the pressure of the backfill body monitored at the distance of 15 m and 40 m from the coal face is 3.5 MPa and 5.5 MPa respectively. According to the calculation of coal face advancing 4.8 m a day at most, the time of advancing 15 m and 40 m is 3.13 days and 8.33 days respectively, so according to relevant Chinese standards, 3 days, 7 days and 28 days are selected as the curing time of specimens in each test group.

5.3 Analysis of test results

5.3.1 Strength characteristics of the specimen

Through uniaxial compression of the specimens in each test group, the compressive strength is plotted as shown in Fig.13.

From the analysis of Fig.13, it can be seen that the strength of the specimens in each test group showed different degrees of increasing trends with the increase of time. The strength of the specimens in No.1 test group is the least obvious change with time, that is, after adding 30% fly ash into the gangue, the compressive strength is still very small, basically no more than 1 MPa, so the material of No.1 test group cannot be directly used as the support material for roadside backfill bodies.

The components of the test pieces in No. 2-3 test groups are gangue + 5% cement and gangue + 10% cement respectively. As can be seen from Fig.13, the uniaxial compressive strength of the specimens is significantly higher than that of the No. 1 test group, especially in the period from 7 days to 28 days, the strength increase is relatively large, but compared with the theoretical strength under the corresponding time, it is still small, that is, the roadside backfill body with this material ratio cannot effectively resist the ground pressure behaviors in the coal face advancement in time. Therefore, the materials with the ratio of No. 2-3 test groups cannot be directly used as theoretical support materials for roadside backfill body.

Different proportions of cement were added to the materials of No. 1 test group to form test specimens of No. 4-6 test group. It can be seen from Fig.13 that the compressive strength of the specimens also obviously increases with the increase of cement content, indicating that cement and fly ash react with each other to jointly promote the cementation of the backfill body and improve the bearing capacity of the gangue cemented body. Among them, the strength of the backfill body formed by the material ratio of the No. 6 test group is the highest. The strength at the curing time of 3 days and 7 days is 4.0 MPa and 6.5 MPa, respectively, which are greater than the theoretical roof pressure of 3.5 MPa and 5.5 MPa at 3.13 days and 8.33 days behind the coal face, respectively. In addition, the strength of the specimens in the No. 6 test group after 7 days is still increasing, which is always greater than the peak value of ground pressure in engineering practice. Therefore, the roadside backfill body with the material ratio of the No. 6 test group can always resist the overburden subsidence during the advancement of the coal face, and can stably support the roof pressure. The strength of the specimen with this material ratio meets the theoretical requirements.

5.3.2 Deformation and failure characteristics

To analyze the deformation and failure characteristics of the specimens in the No. 6 test group under different time conditions, the stress-strain compression curve and the failure morphology after compression are shown in Fig.14.

In Fig.14, it can be seen that the shape of the stress-strain curve of the backfill specimen is similar to that of the typical rock stress-strain curve, but the failure stage of the specimen is different. The post-peak failure process of the specimen with a curing time of 3 days is relatively slow, the top of the stress-strain curve changes smoothly, the strain in the post-peak failure stage increases continuously, and the residual strength shows a downward trend in volatility until the specimen is completely destroyed. However, the specimens with curing time of 7 days and 28 days have a sharper top shape of the stress-strain curve due to crack expansion and instability failure occurred faster during the compression process, and the curve of the post-peak failure stage has a sharp downward trend, indicating that the specimens with a long curing time have higher strength and greater hardness, once the pressure exceeds their peak strength, they will suddenly lose stability and damage, so that the failure form of the specimens with long curing time and high compressive strength tends to develop towards brittle failure. The strain range of the specimens with different curing times when they fail is between 0.03-0.045. The strain for the initial failure of the specimen with a curing time of 3 days after reaching the peak strength is about 0.035-0.04, and the strain at the final instability failure is about 0.06-0.065, indicating that the final deformation of the backfill body with short curing time and low compressive strength is greater than that of the backfill body with long curing time and high compressive strength, but the overall deformation of the backfill body is still small during the compression process.

Analyzed from the failure morphology of the specimen, whether the curing time is 3 days, 7 days or 28 days, before the specimen is completely destroyed, it is accompanied by the process of deformation, crack initiation, and crack development. The specimens generally have splitting failure modes, the surface of the specimen mostly has several wide longitudinal main cracks, accompanied by multiple longitudinal secondary cracks, which extend from top to bottom and jointly cause damage to the whole specimen. Observing the specimens, it is found that, compared with the specimens in the initial state, the specimens after the destruction have generally had obvious deformation such as compression and expansion, while the surface of the specimen did not appear loose and collapsed in a large area, the area where the blocks spalling mostly occurs in the upper part of the specimen. Moreover, when the specimens with long curing time and high strength are damaged, there are relatively few cracks and spalling blocks, and the integrity and stability of the damaged specimens are relatively good.

6. Discussion

In this paper, the ground pressure during the backfilling process was monitored and analyzed in Xingtai Mine as an engineering example, and the spatiotemporal law of ground pressure behavior and overlying strata subsidence in the solid backfilling stope of Xingtai Mine is verified by similar material simulation. Based on these, the spatiotemporal coupling model of ground pressure behavior, roof subsidence and

backfill reinforcement is established, and the theoretical requirements for the bearing performance of roadside backfill bodies are put forward to guide the selection and ratio of backfill materials. Finally, through the mechanical property test of the backfill materials, the material ratio which meets the theoretical requirements and is suitable for roadside backfilling in Xingtai Mine is obtained. Compared with the traditional backfill material proportioning method, this paper puts forward the targeted strategy of roof controlling for gob-side entry retaining in backfilling mining, that is, the ratio of backfill materials and the mechanical properties of backfill body are determined through the stope ground pressure behavior law in the backfilling process, so as to avoid the blindness of material selection and roadside backfilling, such as blindly adding cement into the backfill material to improve the strength, resulting in the increase of roadside backfilling cost, etc. The idea and method of determining the material ratio and mechanical properties of roadside backfill bodies according to the ground pressure behavior can guide the engineering practice of gob-side entry retaining in backfilling mining under similar conditions.

However, there are still some limitations in this paper. First, the roof structure above the coal seam in Xingtai Mine is complete and in good condition. Regardless of the ground pressure, roof subsidence and the compression of the roadside backfill body, the roof conditions of the mine are favorable for gob-side entry retaining in backfilling mining. However, the stope roof in many mines is weak and broken, the ground pressure appearance degree is different, and the roof subsidence has no obvious regularity, resulting in high safety risk of stope backfilling, and it is also very difficult to retain and maintain the roadside backfill body. According to the relevant literature, there is no successful case of gob-side entry retaining in backfilling mining under the condition of weak and broken roof. Therefore, the poor geological conditions greatly limit the application of roadside backfilling. Second, in the process of backfill material selection and proportioning, the proportion of cement in the backfill materials meeting the theoretical strength requirements reaches 10%, accounting for a large proportion and a large amount. In the actual project of gob-side entry retaining, most of the cement used by coal enterprises needs to be purchased, and the price of cement is higher than that of solid waste materials. Therefore, more cement consumption will increase the cost of roadway retaining and reduce the backfill benefit, thereby reducing the willingness of coal enterprises to adopt backfilling mining. Moreover, the strength and compressive strain of the backfill specimen are obtained under ideal laboratory conditions, the curing temperature and humidity are constant, and the specimen size is small. These factors have an impact on the increase of strength. However, the underground environment is complex, and there will be large errors in the on-site material proportioning operation process. If the backfill body with this material ratio is manufactured and compressed under the complex underground environment, its size is large, its shape is irregular, and its mechanical properties may be greatly reduced, thus reducing the support effect of the roadside backfill body with this material ratio. Therefore, the backfill material with this ratio is still lack of field test and application to verify and optimize it.

The limitation of this paper is the direction of future research. In the future, it is important content to develop the technology of gob-side entry retaining in backfilling mining which can adapt to the harsh underground geological conditions. For example, under the condition of broken roof, the cooperative control roof mode of constructing support walls in roadside and fluid grouting in goaf can be used to gob-side

entry retaining. Moreover, it is necessary to enrich the types and the sources of backfill materials, and adopt cementitious materials that can replace cement with wider sources and lower cost, such as increasing the fly ash content and properly adding desulfurization gypsum, so as to improve the economy and practicability of roadside backfilling. Finally, based on the research of high-quality and low-cost roadside backfill materials, the backfill materials are applied to the roadside backfilling engineering practice, and the mechanical properties of roadside backfill body are compared with the experimental results in the laboratory, so as to optimize the composition and ratio of backfill materials. This is a very important research content in the future.

7. Conclusions

(1) The engineering practice of dense solid backfilling mining carried out in Xingtai Mine shows that as the coal face advances, the first weighting of the roof is not obvious, and the periodic weighting strength is weak. Through pressure monitoring, it can be seen that as the advancing distance increases, the pressure on the backfill body first increases and then stabilizes, the pressure reaches a peak value of 5.5 MPa at 40 m from the coal face, and then the pressure basically stabilizes.

(2) Similar simulation experiments are used to verify the spatiotemporal characteristics of ground pressure in dense backfilling mining, it shows that as the backfill distance and time increase, the roof stress has undergone a changing process of “stress rise-stress unloading-stress recovery and then stress stability”, while as the backfill body is far away from the coal face, the force on the goaf backfill body continues to increase until it is stable. The stress and displacement distributions of the roof and the backfill body are low near the coal pillar and high in the middle of the backfilling area.

(3) The spatiotemporal coupling model between roof subsidence and backfill body reinforcement is constructed based on the spatiotemporal law of ground pressure behavior obtained from the engineering practice and similar material modeling, and the theoretical requirements for the bearing capacity of roadside backfill body under conditions of gob-side entry retaining in backfilling mining are put forward.

(4) Through material ratio and compression experiments, the aging strength of the backfill materials at various ratios was studied, and finally the optimal ratio of backfill materials that met the theoretical requirements was obtained as gangue: fly ash: cement=10:3: 1. and its deformation and failure characteristics are analyzed.

Declarations

Data Availability

All data and models generated or used during the study are available within the article. Some data and models referred to the previous research by Liu et al.(2010) and Talbol (1907) which have been cited in the text.

Conflicts of Interest

The authors declare that they have no conflicts of interest.

Funding

This research was supported by China National Key Research and Development Program (2019YFC1904304) , Key R&D Program Projects in Hebei Province(18273815D) and Research Project of Energy Research Institute of Hefei Comprehensive National Science Center (21KZS217).

References

Chang QL, Tang WJ, Xu Y, Zhou HQ (2018) Research on the width of filling body in gob-side entry retaining with high-water materials. *International Journal of Mining Science and Technology* 28:519-524. doi:10.1016/j.ijmst.2017.12.016.

Chen L, Zheng ZY, Xu XQ, Zhao J (2018) Relationship between the strength formation rate of the backfill body and the advancing speed of the coal face, *J Min Sci Tech* 3(2):156-164 doi: 10.19606/j.cnki.jmst.2018.02.007

Cheng LC, Qin YL, Li XW, Zhao XY (2020) A Laboratory and Numerical Simulation Study on Compression Characteristics of Coal Gangue Particles with Optimal Size Distribution Based on Shape Statistics. *Math Probl Eng* 2020:13. doi:10.1155/2020/8046156

Fuller WB, Thompson SE (1907) The laws of proportioning concrete, *Transactions of the American Society of Civil Engineers* 59(2):67–143. <https://doi.org/10.1061/TACEAT.0001979>

Gong P, Ma ZG, Ni XY, Zhang RR (2018) An Experimental Investigation on the Mechanical Properties of Gangue Concrete as a Roadside Support Body Material for Backfilling Gob-Side Entry Retaining. *Advances in Materials Science and Engineering* 2018:11. doi:10.1155/2018/1326053

Gong P, Ma ZG, Zhang RRC, Ni XY, Liu F, Huang ZM (2017) Surrounding Rock Deformation Mechanism and Control Technology for Gob-Side Entry Retaining with Fully Mechanized Gangue Backfilling Mining: A Case Study. *Shock Vib* 2017:15. doi:10.1155/2017/6085941

Huang J, Tian CY, Xing LF, Bian ZF, Miao XX (2017) Green and sustainable mining: underground coal mine fully mechanized solid dense stowing-mining method, *Sustainability* 9(8): 1-18. doi: 10.3390/su9081418

Huang YL, Zhang JX, Zhang Q, Zan DF. Technology of gob-side entry retaining on its original position in fully-mechanized coalface with solid material backfilling, *J China Coal Soc* 10(10): 1624-1628. doi: 10.13225/j.cnki.jccs.2011.10.024

Ju F, Chen ZW, Zhang Q, Huang P, Tai Y, Lan LX (2015) Surrounding rock stability control in gob-side entry retaining with solid backfilling in coal mining technology, *J Min & Safety Eng* 32(6):936-942 doi: 10.13545/j.cnki.jmse.2015.06.011

- Li HZ, Guo GL, Zha JF (2017) Study on time-varying characteristics of similar material model strength and the regulation measures. *Environ Earth Sci* 76:11. doi:10.1007/s12665-017-6857-5
- Li M, Zhang JX, Huang YL, Zhou N (2017) Effects of particle size of crushed gangue backfill materials on surface subsidence and its application under buildings. *Environ Earth Sci* 76:12. doi:10.1007/s12665-017-6931-z
- Li J, Yin ZQ, Li Y, Li CM (2019) Waste rock filling in fully mechanized coal mining for goaf-side entry retaining in thin coal seam. *Arab J Geosci* 12:509. doi:10.1007/s12517-019-4650-3
- Li XW, Zhao XY, Cheng LC, Qin YL (2020) Study on Spatiotemporal Evolution Law of Strata Behaviors in Compacted Backfill, *Chinese J Rock Mech Eng* 39(2):341-348 doi: 10.13722/j.cnki.jrme.2019.0780
- Liu JG, Zhao QB (2010) Coal mining technology with fully mechanized solid backfilling under the building structures in Xingtai Mine, *Coal Sci Tech* 38(3):18-21 doi: 10.13199/j.cst.2010.03.24.liujg.023
- Ma ZG, Gong P, Fan JQ, Geng MM, Zhang GW (2011) Coupling mechanism of roof and supporting wall in gob-side entry retaining in fully-mechanized mining with gangue backfilling, *Min Sci Technol (China)*. 21(6):829-833 doi: 10.1016/j.mstc.2011.05.036
- Miao XX, Zhang JX, Feng MM (2008) Waste-backfill in fully-mechanized coal mining and its application, *J China Univ Min Tech* 18(4):479-482 doi:10.1016/S1006-1266(08)60279-5
- Sun YN, Zhang PS, Yan W, Yan FQ, Wu JD (2019) Experimental study on pressure-bearing deformation characteristics of crushed sandstone in gob, *Coal Sci Tech* 47(12): 56-61 doi: 10.13199/j.cnki.cst.2019.12.008
- Xie SR, Zhang GC, He SS, Sun YJ, Li EP, Yang LG (2014) Surrounding rock control mechanism and its application of gobside retaining entry in deep backfill with large mining height, *J China Coal Soc* 39(12): 2362-2368. doi:10.13225/j.cnki.jccs.2014.0095
- Xu JM, Zhang JX, Huang YL, Ju F (2011) Experimental research on the compress deformation characteristic of waste fly ash and its application in backfilling fully mechanized coal mining technology, *J Mini Safety Eng* 28(1):158-162 (in Chinese)
- Yang DL, Li JP, Du CL, Zheng KH, Liu SY (2017) Particle size distribution of coal and gangue after impact-crush separation, *J Cent South Univ* 24(6):1252-1262 doi:10.1007/s11771-017-3529-2.
- Yang J, He MC, Cao C (2019) Design principles and key technologies of gob side entry retaining by roof pre-fracturing, *Tunn and Undergr Sp Tech* 90:309-318. doi:10.1016/j.tust.2019.05.013.
- Zhang N, Yuan L, Han CL, Xue JH, Kan JG (2012) Stability and deformation of surrounding rock in pillar less gob-side entry retaining, *Safety Sci* 50(4):593-599 doi: 10.1016/j.ssci.2011.09.010

Zhang JX, Jiang HQ, Miao XX, Zhou N, Zan DF (2013) The rational width of the support body of gob-side entry in fully mechanized backfilling mining, *J Min & Safety Eng* 30(2):159-164 (in Chinese)

Zhao XY, Li XW, Yang K, Wei Z (2021) The Spatiotemporal Characteristics of Coupling Effect between Roof and Backfill Body in Dense Backfill Mining, *Geofluids*, 2021: 6684237.

<https://doi.org/10.1155/2021/6684237>.

Zhou BJ, Xu JH, Zhao MS, Zeng QL (2012) Stability study on naturally backfill body in gob-side entry retaining, *Int J Min Sci Tech* 22(3):423-427 doi: 10.1016/j.ijmst.2012.01.001

Figures

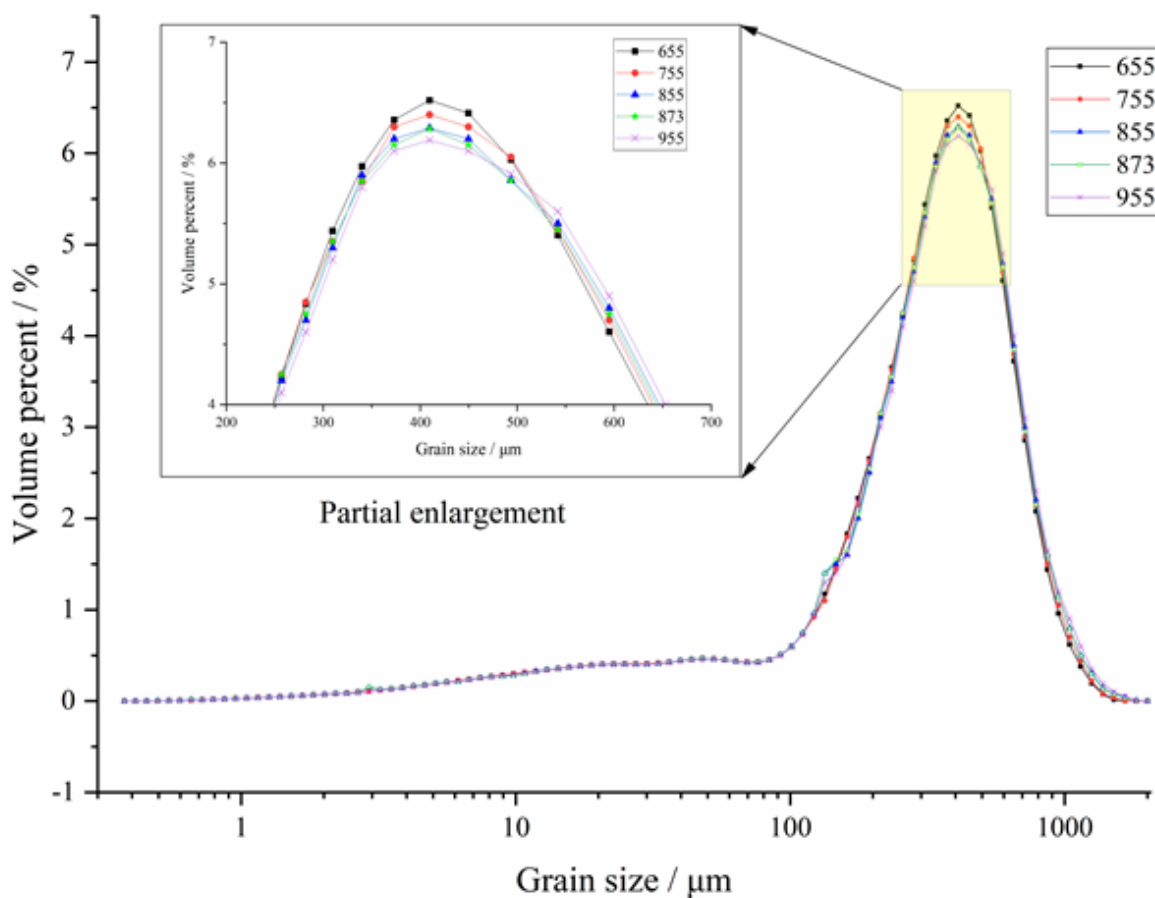


Figure 1

Grain size distribution curve of similar materials with different ratio numbers

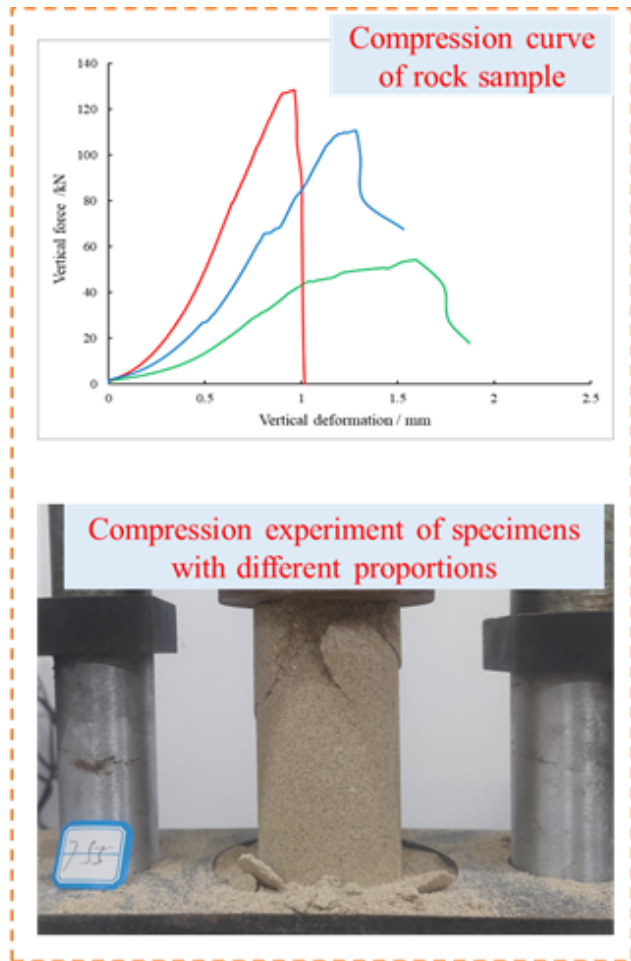
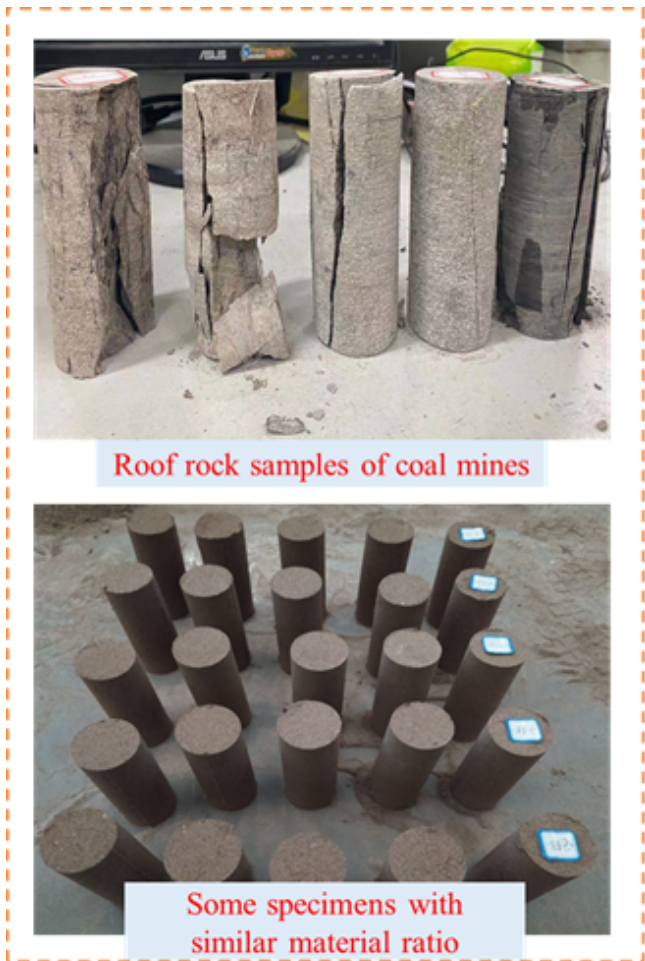


Figure 2

Similar material ratio experiment

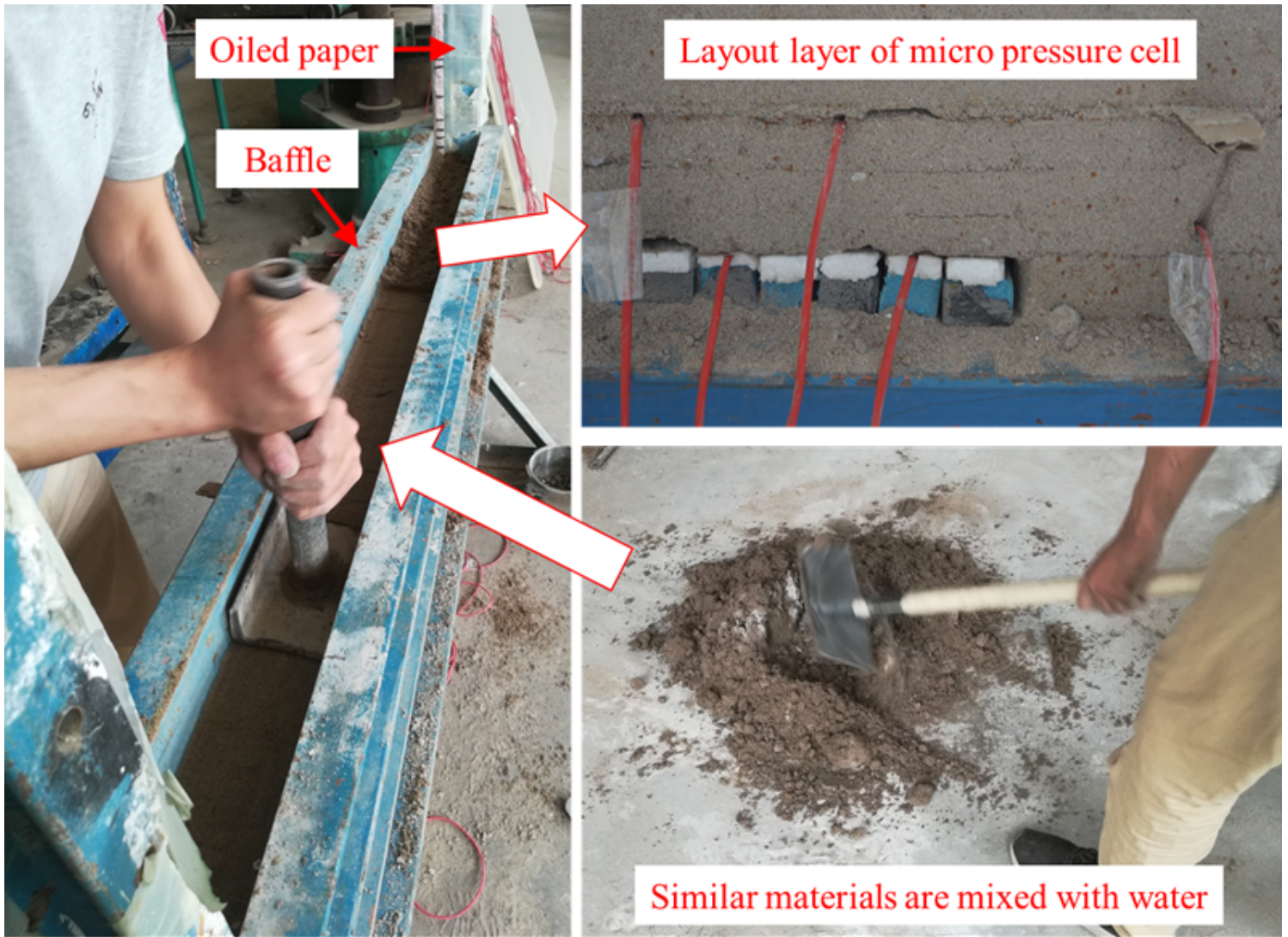


Figure 3

Construction of the similar material model

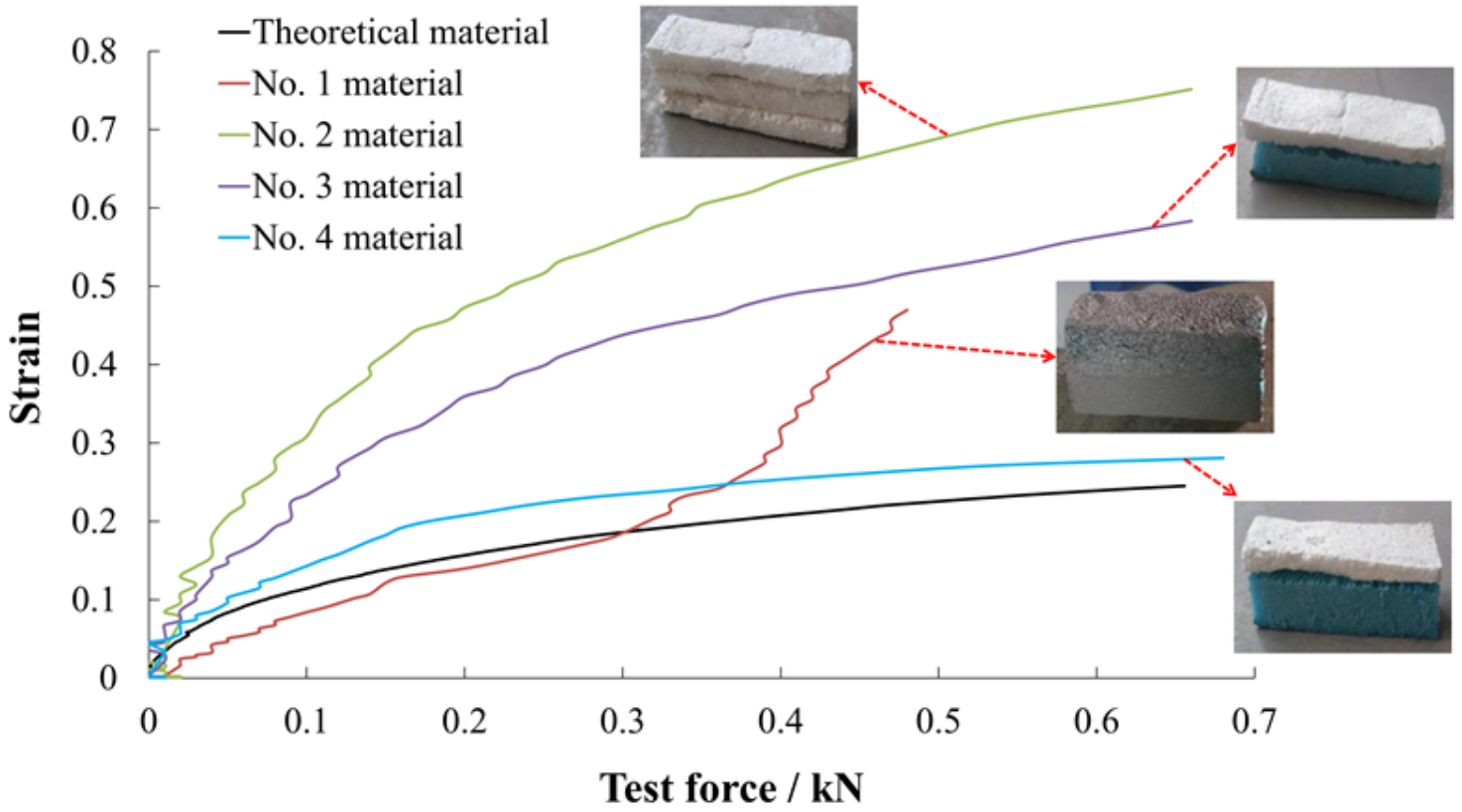


Figure 4

Compression characteristic curve of four combined materials

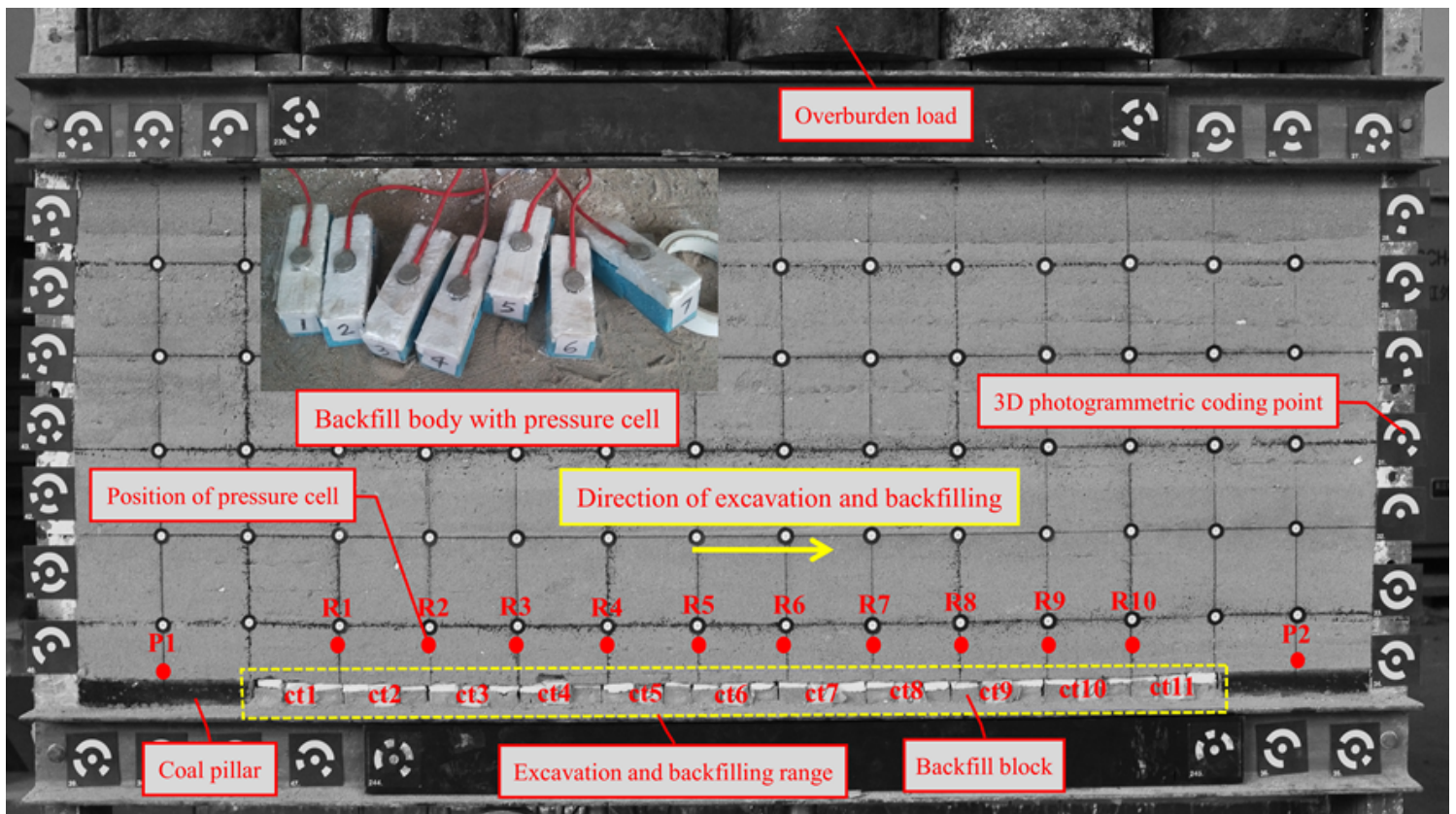


Figure 5

The layout of measuring points in the model

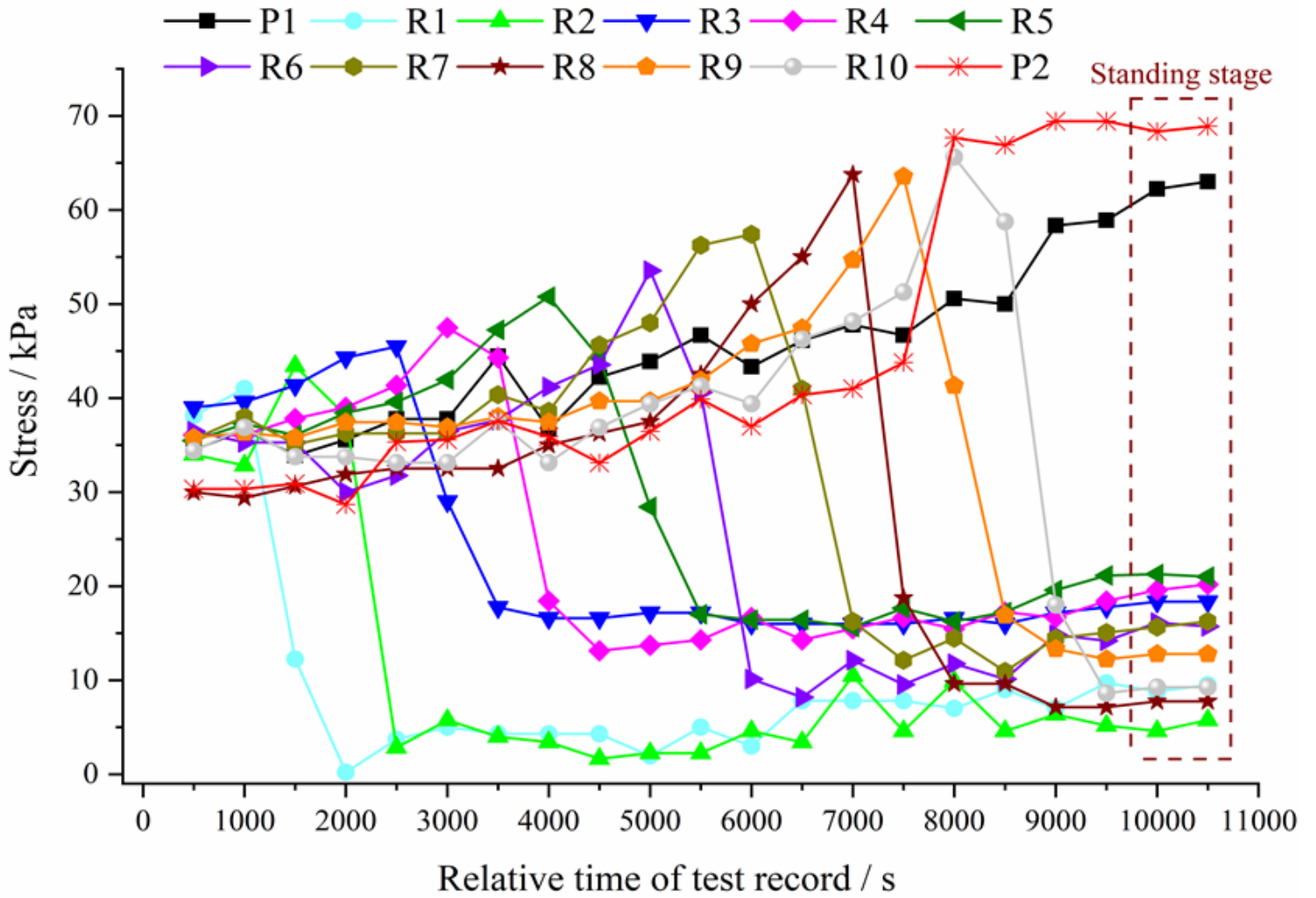


Figure 6

Stress record of roof measuring points

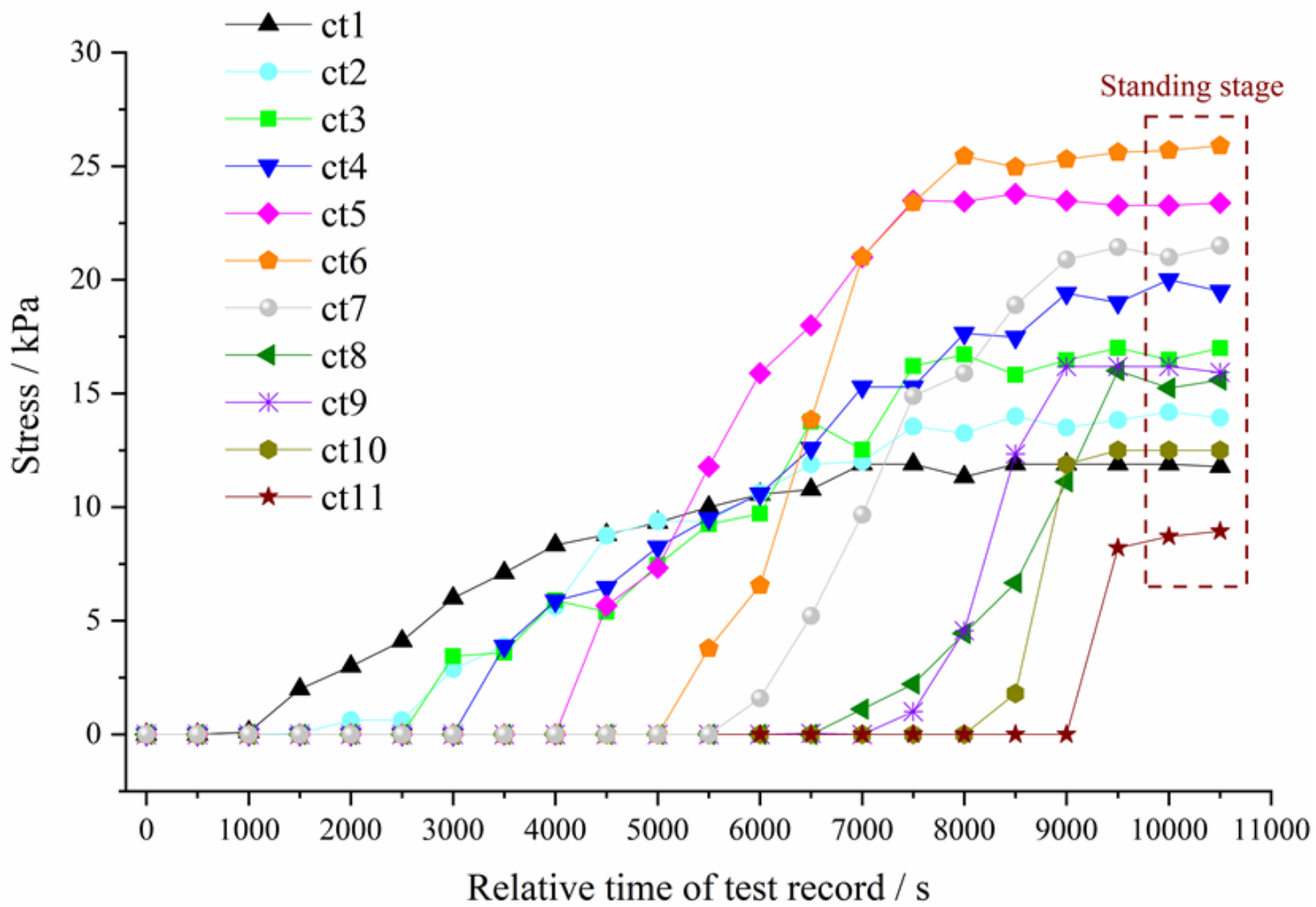


Figure 7

Stress record of measuring points on backfill body

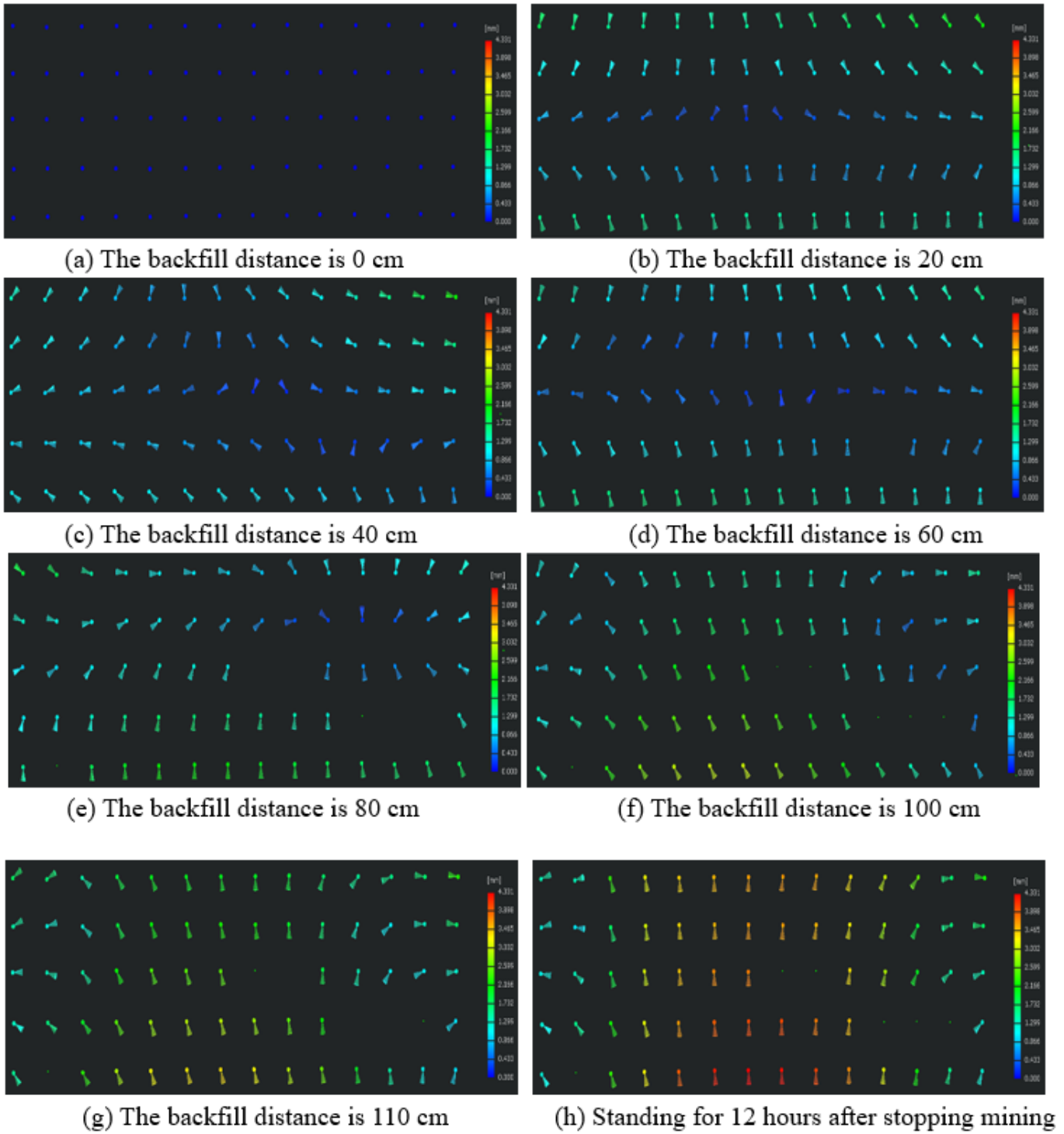


Figure 8

Deformation diagram of overlying strata

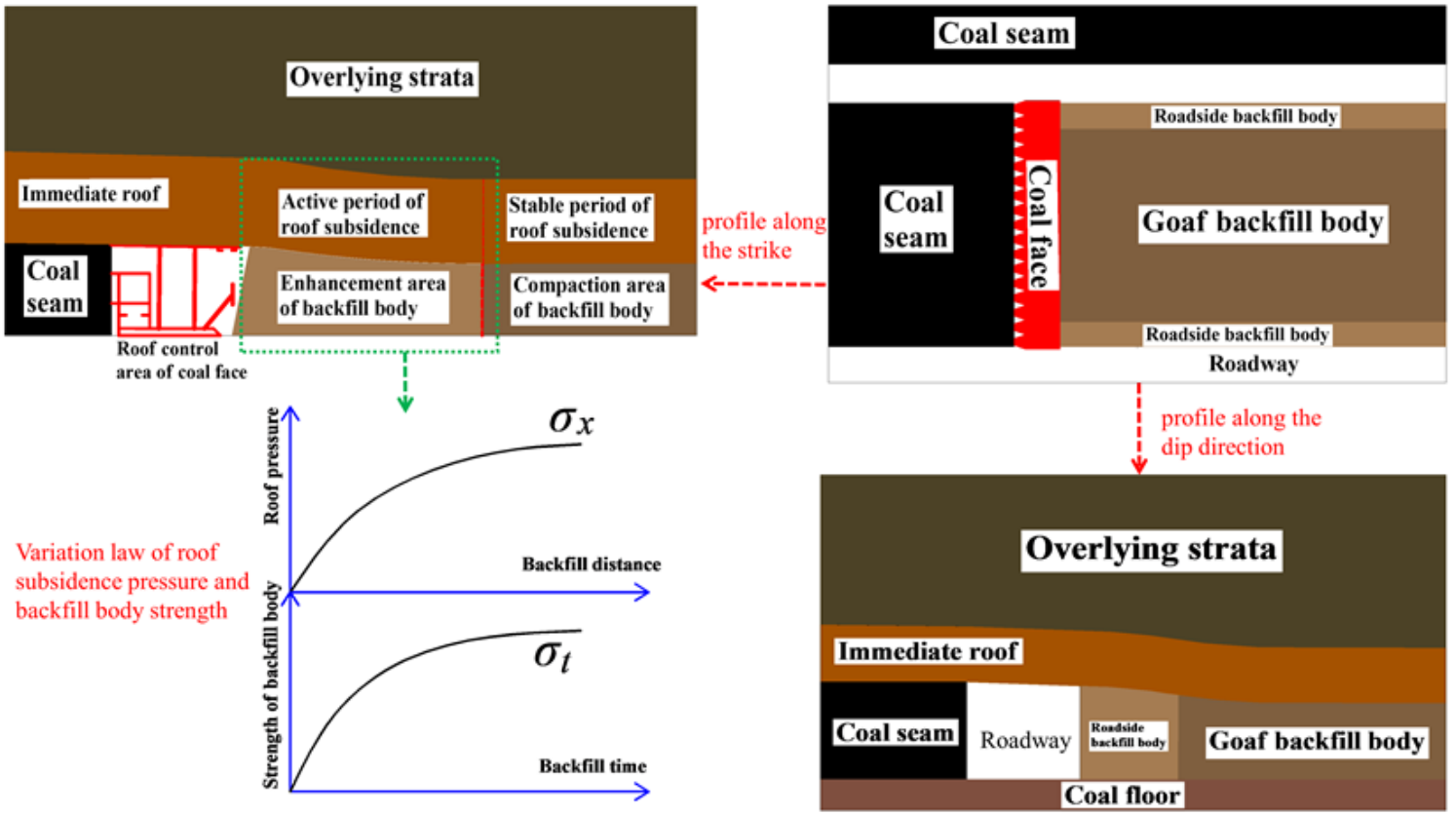


Figure 9

Spatiotemporal coupling model of roof and backfill body

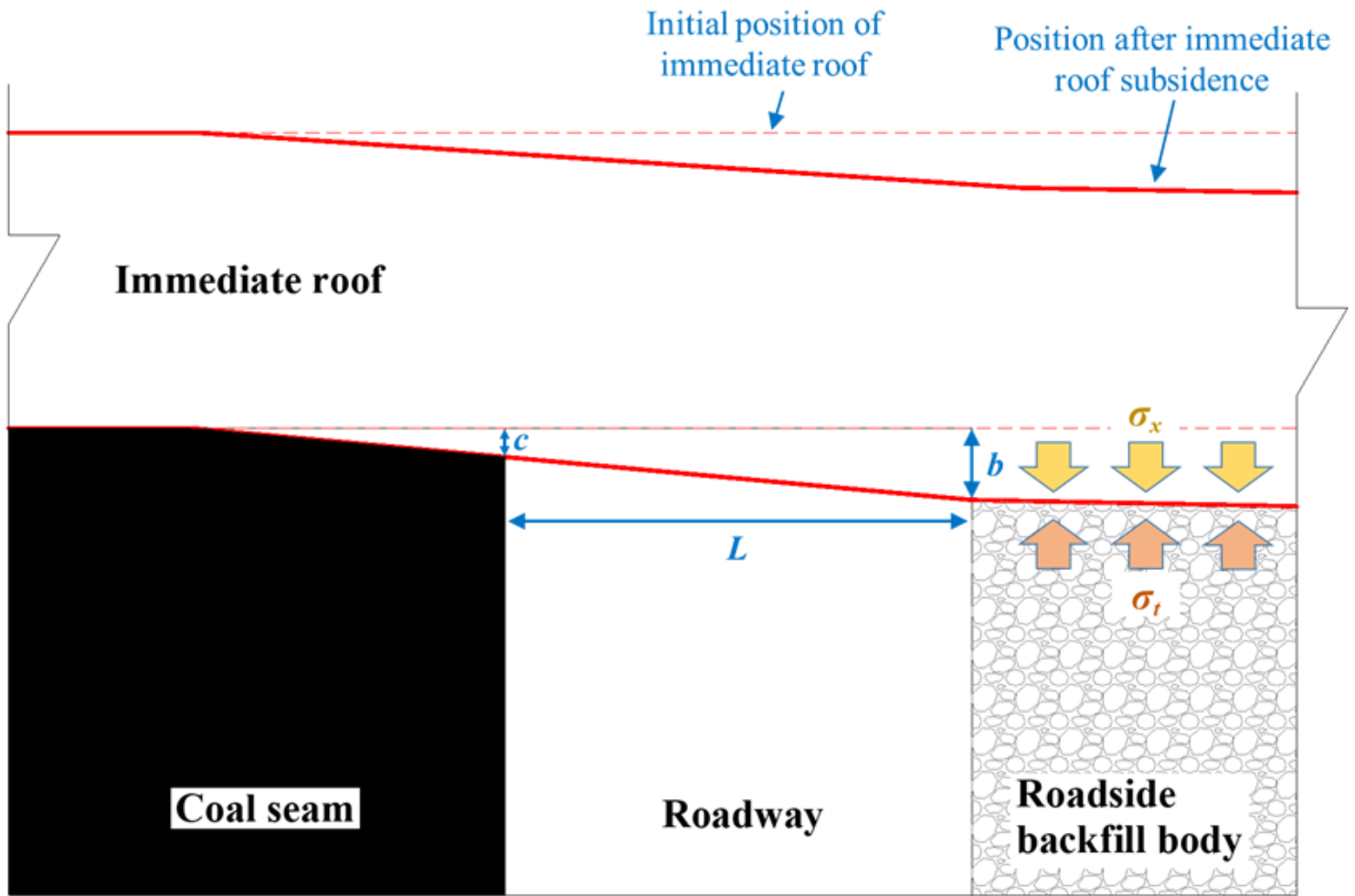


Figure 10

Cross-section of the roadway before and after immediate roof subsidence

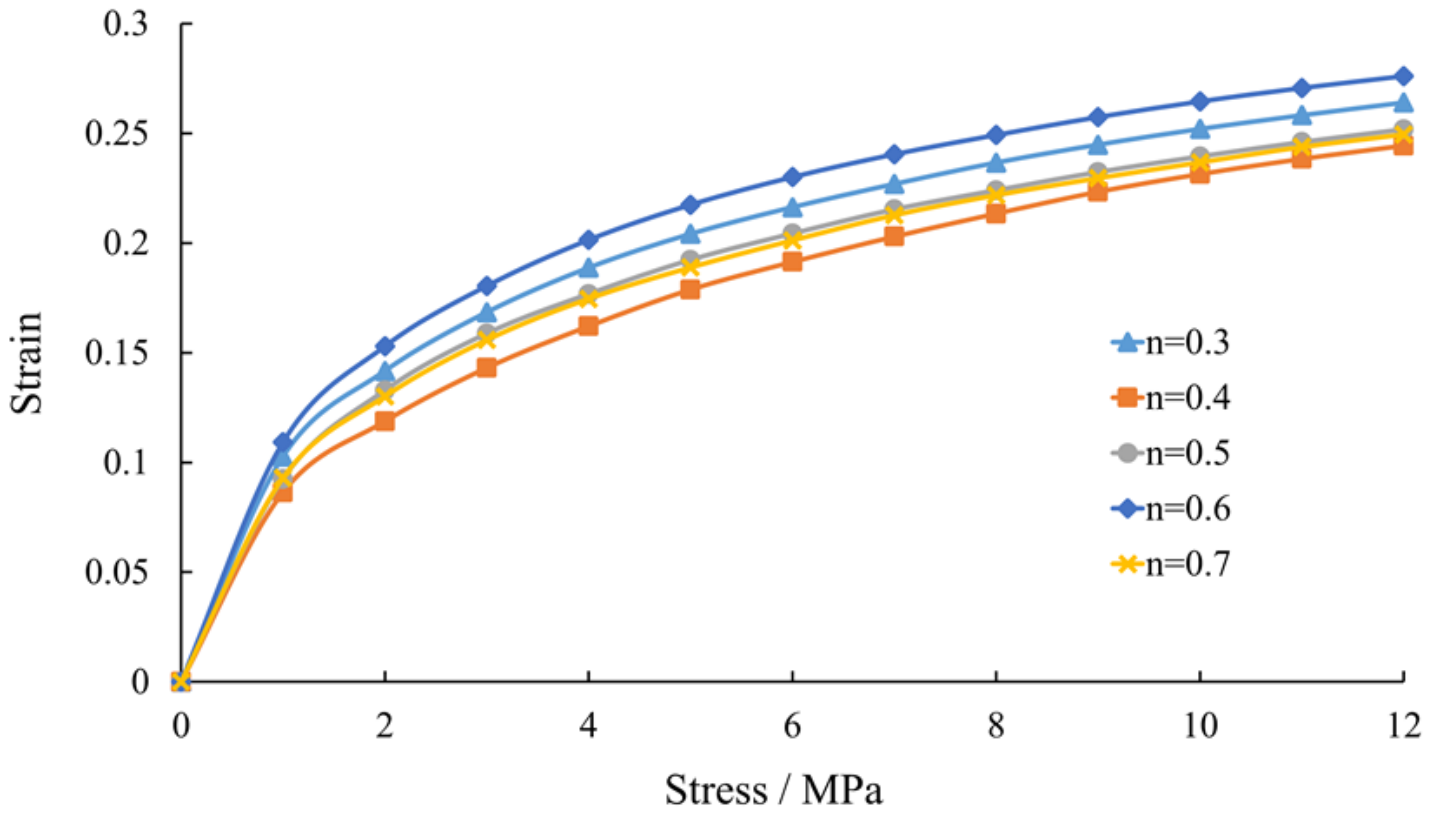


Figure 11

Compressive stress-strain curve of continuously graded gangue



(a) Gangue material

(b) Fly ash material

(c) Cement materials

Figure 12

Test materials

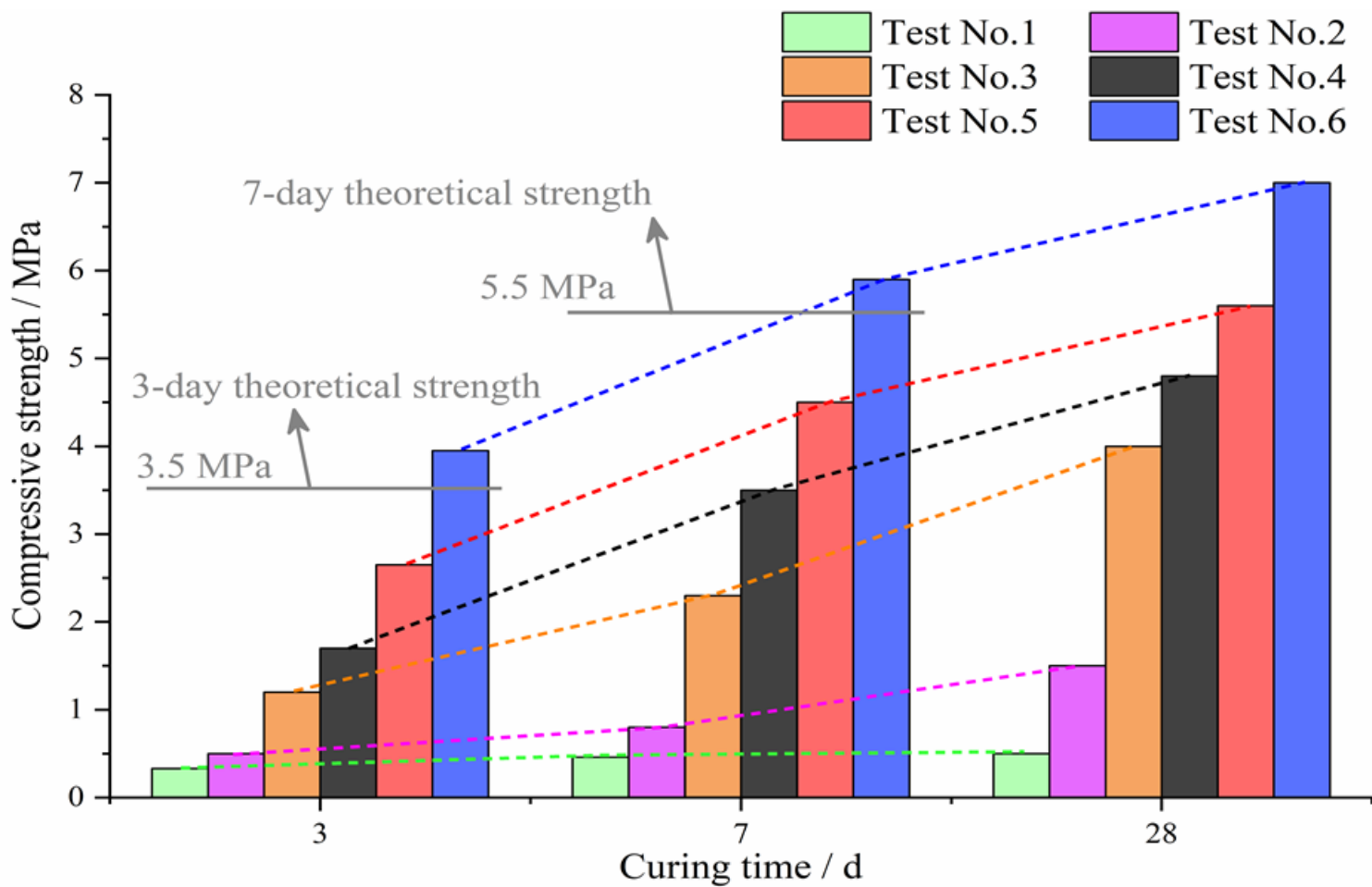


Figure 13

Compressive strength of specimens

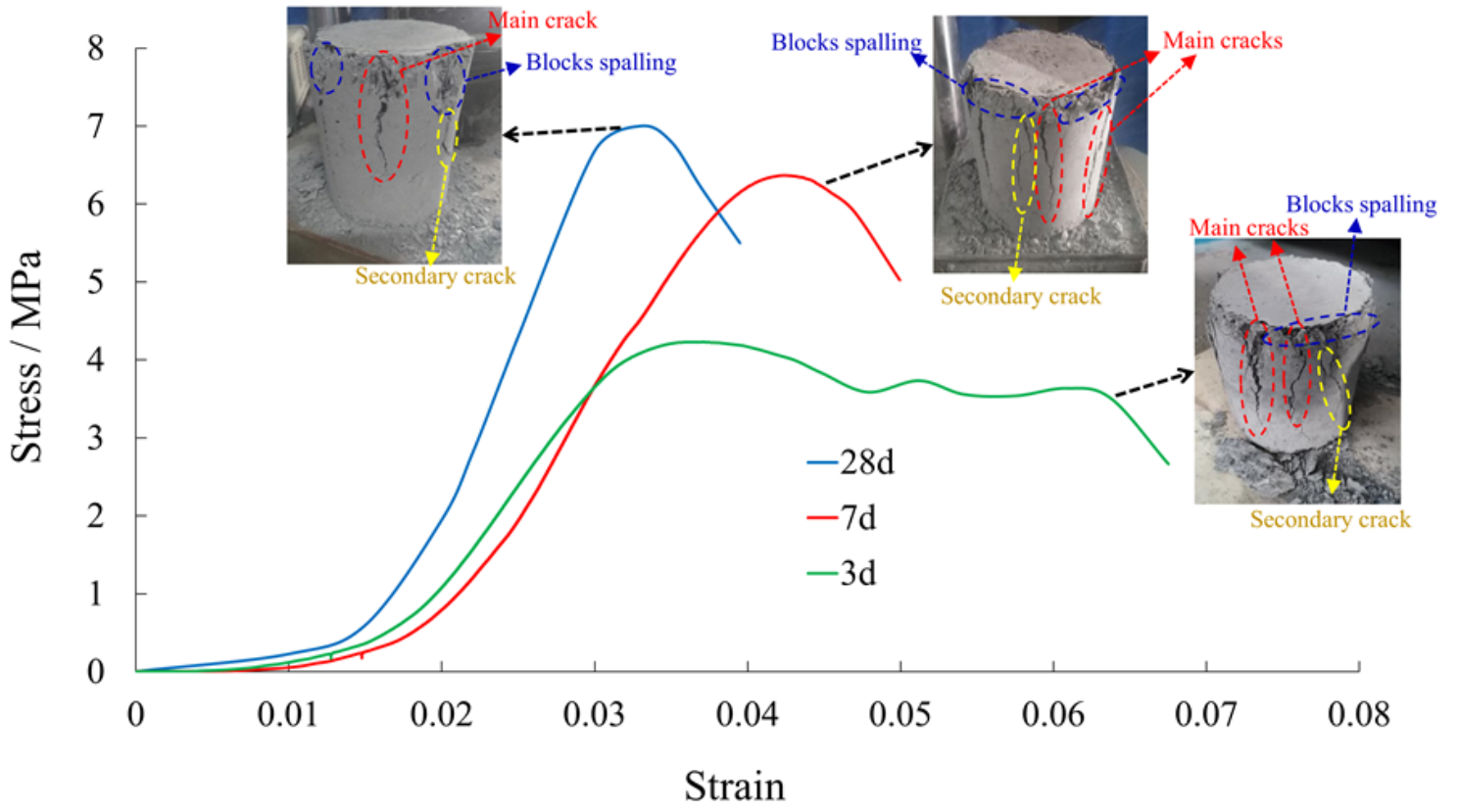


Figure 14

Deformation characteristic curve and failure morphology of the specimen